Direct Observation of Optically Forbidden Energy Transfer between CuCl Quantum Cubes via Near-Field Optical Spectroscopy

Tadashi Kawazoe,[1] Kiyoshi Kobayashi,[1] Jungshik Lim,[2] Yoshihito Narita,[3] and Motoichi Ohtsu[1,2]

[1]*Exploratory Research for Advanced Technology, Japan Science and Technology Corporation,*
687-1 Tsuruma, Machida, Tokyo 194-0004, Japan
[2]*Interdisciplinary Graduate School of Science and Engineering, Tokyo Institute of Technology,*
4259 Nagatsuta, Midori-ku, Yokohama 226-8502, Japan
[3]*JASCO Corporation, 2967-5, Ishikawa-cho, Hachioji, Tokyo, 192-8537, Japan*
(Received 3 July 2001; published 25 January 2002)

We report, for the first time, evidence of near-field energy transfer among CuCl quantum cubes using an ultrahigh-resolution near-field optical microscopy and spectroscopy in the near UV region at 15 K. The sample was high-density CuCl quantum cubes embedded in a NaCl matrix. Measured spatial distributions of the luminescence intensities from 4.6-nm and 6.3-nm quantum cubes clearly established anticorrelation features. This is thought to be a manifestation of the energy transfer from the lowest state of exciton in 4.6-nm quantum cubes to the first dipole-forbidden excited state of exciton in 6.3-nm quantum cubes, which is attributed to the resonant optical near-field interaction.

Observations of a single quantum dot have recently become possible using near-field optical spectroscopy [1,2] and microluminescence spectroscopy [3,4]. Spectroscopy of individual quantum dots is one of the most important topics of nanostructure physics, and several extraordinary phenomena have been reported, such as intermittent luminescence [5] and long coherent time [6]. The coupled quantum-dots system exhibits more unique properties (e.g., the Kondo effect [7,8], Coulomb blockade [9,10], and breaking the Kohn theorem [11]) in contrast with the single quantum-dot system. The quantum dots system reveals a variety of interactions such as carrier tunneling [7–10], Coulomb coupling [11], spin interaction [12], and so on. Investigation of interactions among quantum dots is important not only for deep understanding of the various physical phenomena but also for developing novel functional devices [7–12]. The optical near-field interaction [1] is of particular interest, as it can govern the coupling strength among quantum dots.

Recently, Mukai *et al.* reported ultrafast "optically forbidden" energy transfer from an outer ring of loosely packed bacteriochlorophyll molecules, called B800, to an inner ring of closely packed bacteriochlorophyll molecules, called B850, in the light-harvesting antenna complex of photosynthetic purple bacteria [13]. They theoretically showed that this transfer is possible when the point transition dipole approximation is violated due to the size effect of B800 and B850. From our viewpoint, this energy transfer is due to the optical near-field interaction between B800 and B850. Similarly, the energy can be transferred from one dot to another by the optical near-field interaction for the quantum dots system, even if it is a dipole-forbidden transfer.

CuCl quantum cubes (QCs) embedded in NaCl have the potential to be an optical near-field coupling system

that exhibits this optically forbidden energy transfer. This is because, for this system, another possibility of energy transfer, such as carrier tunneling, Coulomb coupling, and so on, can be neglected, because carrier wave function is localized in QCs due to a deep potential depth of more than 4 eV and the Coulomb interaction is weak due to small exciton Bohr radius of 0.68 nm. Conventional optical energy transfer is also negligible, since the energy levels of nearly perfect cubic CuCl QCs are optically forbidden, and are confined to the energy levels of exciton with an even principal quantum number [14]. However, Sakakura *et al.* observed the optically forbidden transition in a hole-burning experiment using CuCl QCs [15]. Although they attributed the transition to an imperfect cubic shape, the experimental and simulation results did not show such imperfection. We believe that the transition was due to the energy transfer between the CuCl QCs, via the optical near-field interaction similar to the optically forbidden energy transfer between B800 and B850 in the above-mentioned photosynthetic system. Thus far, this type of energy transfer has not been directly observed. This Letter reports the direct observation of energy transfer from the exciton state in a CuCl QC to the optically forbidden exciton state in another CuCl QC by optical near-field spectroscopy.

It is well known that translational motion of the exciton center of mass is quantized due to the small exciton Bohr radius for CuCl quantum dots, and that CuCl quantum dots become cubic in a NaCl matrix [15–17]. The potential barrier of CuCl QCs in a NaCl crystal can be regarded as infinitely high, and the energy eigenvalues for the quantized Z_3 exciton energy level (n_x, n_y, n_z) in a CuCl QC with the side length of L are given by

$$E_{n_x,n_y,n_z} = E_B + \frac{\hbar^2 \pi^2}{2M(L - a_B)^2}(n_x^2 + n_y^2 + n_z^2), \quad (1)$$

where E_B is the bulk Z_3 exciton energy, M is the translational mass of exciton, a_B is its Bohr radius, n_x, n_y, and n_z are quantum numbers ($n_x, n_y, n_z = 1, 2, 3, \ldots$), and $d = (L - a_B)$ corresponds to an effective side length found through consideration of the dead layer correction [15]. The exciton energy levels with even quantum numbers are dipole-forbidden states, that is, optically forbidden [14]. However, the optical near-field interaction is finite for such energy levels [18].

According to Eq. (1), there exists a resonance between the quantized exciton energy level of quantum number $(1, 1, 1)$ for the QCs with effective side length d and the quantized exciton energy level of quantum number $(2, 1, 1)$ for the QCs with effective side length $\sqrt{2}\,d$. For this type of resonant condition, the coupling energy of the optical near-field interaction is given by the following Yukawa function [1,18]:

$$V(r) = A\,\frac{\exp(-\mu r)}{r}. \tag{2}$$

Here r is the separation between two QCs, A is the coupling coefficient, and the effective mass of the Yukawa function μ is given by

$$\mu = \frac{\sqrt{2E_{n_x,n_y,n_z}(E_{\mathrm{NaCl}} + E_{n_x,n_y,n_z})}}{\hbar c}, \tag{3}$$

where E_{NaCl} is the exciton energy of a NaCl matrix. The value of the coupling coefficient A depends on each experimental condition; however, we estimate it from the result of the previous work on the interaction between a Rb atom and the optical near-field probe tip [18]. The value for A for 5-nm CuCl QCs is found to be more than 10 times larger than that for the Rb-atom case, since the coupling coefficient A is proportional to the oscillator strength and square of the photon energy [18,19]. Assuming that the separation r between two QCs is equal to 10 nm, the coupling energy $V(r)$ is the order of 10^{-4} eV. This corresponds to a transition time of 40 ps, which is much shorter than the exciton lifetime of a few ns. In addition, intersublevel transition τ_{sub}, from higher exciton energy levels to the lowest one, is generally less than a few ps and is much shorter than the transition time due to optical near-field coupling [20]. Therefore, most of the energy of the exciton in a CuCl quantum cube with the side length of d transfer to the lowest exciton energy level in the neighboring quantum cubes with a side length of $\sqrt{2}\,d$ and recombine radiatively in the lowest level.

We fabricated CuCl QCs embedded in a NaCl matrix by the Bridgman method and successive annealing, and found the average size of the QCs to be 4.3 nm. The sample was cleaved just before the near-field optical spectroscopy experiment in order to keep the sample surface clean. The cleaved surface of the sample with 100-μm-thick sample was sufficiently flat for the experiment; i.e., its roughness

was less than 50 nm, at least within a few μm squares. A 325-nm He-Cd laser was used as a light source. A double-tapered fiber probe was fabricated by chemical etching and a 150-nm gold coating was applied [21]. A 50-nm aperture was fabricated by the pounding method [22].

The curve in Fig. 1(a) shows a far-field luminescence spectrum of the sample that was recorded with a probe-sample separation of 3 μm in the collection-mode operation [1] of the cryogenic near-field optical microscope at 15 K. It represents the collective luminescence intensity from several CuCl QCs, and is inhomogeneously broadened owing to the size distribution of the QCs. Figure 1(b) represents the differential spectrum, which is the intensity difference between luminescence measured with probe-sample separations of 3 μm and of less than 10 nm. This curve consists of many fine structures. These appear as the contribution of the QCs near the apex of the probe because of the drastic increase in the measured luminescence intensity for a probe-sample separation less than 10 nm. The average density of the QCs is 10^{17} cm^{-3}. Thus, the average separation between the QCs is less than 30 nm, estimated from the concentration of CuCl. Therefore, the spectral peaks in Fig. 1(b), obtained by near-field measurement using the 50-nm aperture fiber probe, originate from several QCs of different size. Among these, the peaks X and Y correspond to the confined Z_3-exciton energy levels of quantum number $(1, 1, 1)$ for the QCs with side lengths (L) of 4.6 and 6.3 nm, respectively. Their effective side lengths d are 3.9 and 5.6 nm, whose size
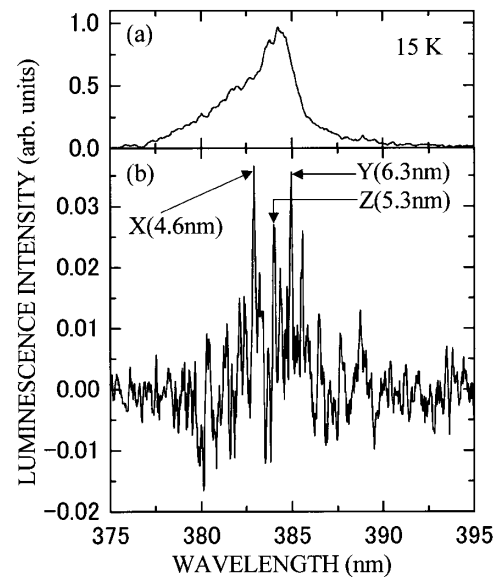
FIG. 1. (a) Far-field luminescence spectrum of a sample recorded with probe-sample separation of 3 μm for the collection-mode operation at 15 K. (b) The differential luminescence spectrum, which is the intensity difference between luminescence measured with the probe-sample separations of 3 μm and of less than 10 nm. X, Y, and Z correspond to the wavelengths of lowest exciton state in quantum cubes with the side lengths of 4.6, 6.3, and 5.3 nm, respectively.

ratio is close to $1:\sqrt{2}$, and thus the $(1,1,1)$ and $(2,1,1)$ quantized exciton levels are resonant with each other to be responsible for energy transfer between the QCs.

Figures 2(a) and 2(b) show the spatial distributions of the luminescence intensity, i.e., near-field optical microscope images, for peaks X and Y in Fig. 1(b), respectively. The spatial resolution, which depends on the aperture diameter of the near-field probe, was smaller than 50 nm. These images clearly establish anticorrelation features in their intensity distributions, as manifested by the dark and bright regions surrounded by white broken curves. In order to confirm the anticorrelation feature more quantitatively, Fig. 3 shows the values of the cross-correlation coefficient C between the spatial distribution of the intensity of the luminescence emitted from the (n_x, n_y, n_z) level of exciton in a QC with 6.3-nm side length and that from the $(1,1,1)$ level in a QC with a different side length L. They have been normalized to that of the autocorrelation coefficient of the luminescence intensity from the $(1,1,1)$ level in a

6.3-nm QC, which is identified by an arrow (1) in Fig. 3. To calculate the values of C, spatial Fourier transform was performed on the series of luminescence intensity values in the chain of pixels inside the region surrounded by the broken white curves in Fig. 2. The large negative value of C identified by an arrow (2) clearly shows the anticorrelation feature between Figs. 2(a) and 2(b), i.e., between the $(2,1,1)$ level in a 6.3-nm QC and the $(1,1,1)$ level in a 4.6-nm QC.

This anticorrelation feature can be understood by noting that these spatial distributions in luminescence intensity represent not only the spatial distributions of the QCs, but also some kind of resonant interaction between the QCs. This interaction induces energy transfer from X cubes ($L = 4.6$ nm) to Y cubes ($L = 6.3$ nm). Interpreting this, most of the 4.6-nm QCs "accidentally" located close to 6.3-nm QCs cannot emit light, but instead transfer the energy to the 6.3-nm QCs. As a result, in the region containing embedded 6.3-nm QCs, the luminescence intensity in Fig. 2(a) from 4.6-nm QCs is low, while the corresponding position in Fig. 2(b) is high. As we mentioned above, it is reasonable to attribute the origin of the

X: L=4.6nm

Y: L=6.3nm

Z: L=5.3nm
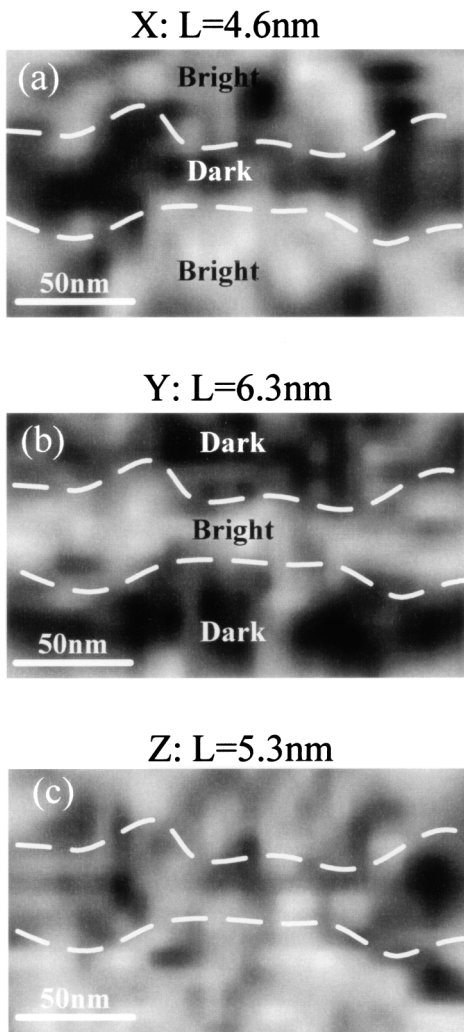
FIG. 2. Spatial distributions of the near-field luminescence intensity for peaks marked as X, Y, and Z in Fig. 1(b), respectively.
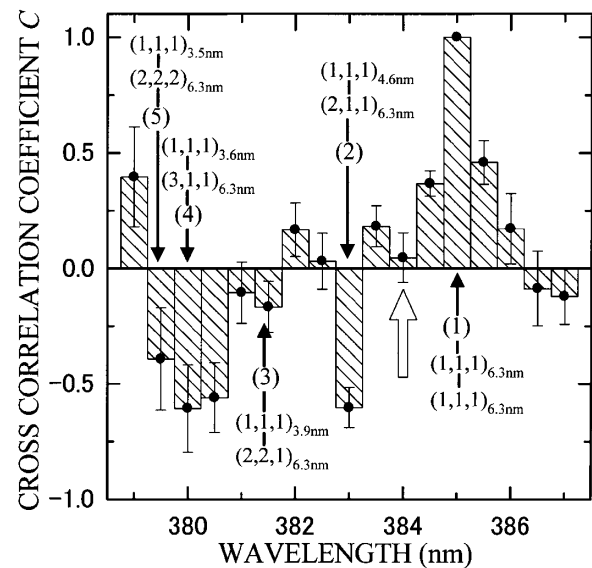
FIG. 3. Values of the cross-correlation coefficient C between the spatial distribution of the intensity of the luminescence emitted from the (n_x, n_y, n_z) level of exciton in a QC with 6.3-nm side length and that from the $(1,1,1)$ level in a QC with the different side length L. They have been normalized to that of the autocorrelation coefficient of the luminescence intensity from the $(1,1,1)$ level in a 6.3-nm QC, which is identified by an arrow (1). The other four arrows (2)–(5) represent the cross-correlation coefficient C between higher levels in a 6.3-nm QC and other sized QCs. They are between (2) the $(2,1,1)$ level in a 6.3-nm QC and the $(1,1,1)$ level in a 3.9-nm QC, (3) the $(2,2,1)$ level in a 6.3-nm QC and the $(1,1,1)$ level in a 3.9-nm QC, (4) the $(3,1,1)$ level in a 6.3-nm QC and the $(1,1,1)$ level in a 3.6-nm QC, and (5) the $(2,2,2)$ level in a 6.3-nm QC and the $(1,1,1)$ level in a 3.5-nm QC. For reference, a white arrow represents the value of C between the $(2,1,1)$ level in a 6.3-nm QC and the nonresonant $(1,1,1)$ level in a 5.3-nm QC.

interaction to the near-field energy transfer. Besides, anti-correlation features appear for every couple of QCs with different sizes satisfying the resonant conditions of the confinement exciton energy levels. Therefore, we claim the first observation of energy transfer between QCs via the optical near field.

For reference, we note the dark area outside the broken curves in Fig. 2(b). This occurs because there are very few 6.3-nm QCs. From the absorption spectrum of the sample, it is estimated that the population of 6.3-nm QCs is one-tenth the population of 4.6-nm QCs. As a result, the corresponding area in Fig. 2(a) is bright due to absence of the energy transfer.

On the other hand, the spatial distributions of the luminescence intensities from other QCs whose sizes do not satisfy the resonant condition given by Eq. (1) did not show any anticorrelation features. This is confirmed by comparing Figs. 2(a), 2(b), and 2(c). Here Fig. 2(c) shows the spatial distribution of the luminescence intensity of peak Z in Fig. 1(b), which corresponds to QCs with a side length of 5.3 nm. The white arrow in Fig. 3 indicates the relationship between Figs. 2(b) and 2(c). The negligibly small value of C identified by this arrow proves the absence of the anticorrelation feature between the exciton energy levels in a 6.3-nm QC and the $(1, 1, 1)$ level in a 5.3-nm QC due to their nonresonant condition.

Furthermore, arrows (3)–(5) also represent clearly large negative values of C, which means the existence of the anticorrelation feature between higher levels in 6.3-nm QC and other sized QCs. They are (3) the $(2, 2, 1)$ level in a 6.3-nm QC and the $(1, 1, 1)$ level in a 3.9-nm QC, (4) the $(3, 1, 1)$ level in a 6.3-nm QC and the $(1, 1, 1)$ level in a 3.6-nm QC, and (5) the $(2, 2, 2)$ level in a 6.3-nm QC and the $(1, 1, 1)$ level in a 3.5-nm QC. These anticorrelation features can also be explained by the resonant optical near-field energy transfer. The features represented by this figure support our interpretation of the experimental results. The large anticorrelation coefficients C identified by arrows (4) and (5) in Fig. 3 are the evidence of multiple energy transfer: Since the $(1, 1, 1)$ levels in 3.5-nm and 3.6-nm QCs resonate or nearly resonate to the $(2, 1, 1)$ level in a 4.6-nm QC, there is another route of energy transfer in addition to direct transfer from the 3.5-nm and 3.6-nm QCs to 6.3-nm QCs, i.e., the transfer via the 4.6-nm QCs. We consider that such multiple energy transfers increase the value of C identified by arrows (4) and (5) in Fig. 3.

In conclusion, CuCl QCs embedded in a NaCl matrix form a system that emphasizes the optical near-field interaction due to its high potential barrier, small radius of exciton, and high density of QCs. Using near-field optical spectroscopic microscopy with a spatial resolution smaller than 50 nm in the near UV region at 15 K, we observed, for the first time, resonant energy transfer occurring from the lowest state of excitons in 4.6-nm QCs to the first dipole-forbidden excited state of excitons in 6.3-nm size QCs. This is attributed to the optical near-field in-teraction between the QCs. In addition, this phenomenon can provide a variety of applications, such as an all-optical near-field switch.

[1] *Near-Field Nano/Atom Optics and Technology,* edited by M. Ohtsu (Springer, Tokyo, Berlin, Heidelberg, New York, 1998).
[2] T. Saiki, K. Nishi, and M. Ohtsu, Jpn. J. Appl. Phys. **37**, 1638 (1998).
[3] J. C. Kim, H. Rho, L. M. Smith, H. E. Jackson, S. Lee, M. Dobrowolska, J. M. Merz, and J. K. Furdyna, Appl. Phys. Lett. **73**, 3399 (1998).
[4] E. Deckel, D. Gershoni, E. Ehrenfreund, D. Spector, J. M. Garcia, and P. M. Petroff, Phys. Rev. Lett. **80**, 4991 (1998).
[5] M. Nirmal, B. O. Dabbousi, M. G. Bawendi, J. J. Macklin, J. K. Trautman, T. D. Harris, and L. E. Brus, Nature (London) **383**, 802 (1996).
[6] N. H. Bonadeo, J. Erland, D. Gammon, D. Park, D. S. Katzer, and D. G. Steel, Science **282**, 1473 (1998).
[7] D. Goldhaber-Gordon, H. Shtrikman, D. Mahalu, D. Abusch-Magder, U. Meirav, and M. A. Kastner, Nature (London) **391**, 156 (1998); D. Goldhaber-Gordon, J. Göres, M. A. Kastner, H. Shtrikman, D. Mahalu, and U. Meirav, Phys. Rev. Lett. **81**, 5225 (1998).
[8] F. Simmel, R. H. Blick, J. P. Kotthaus, W. Wegscheider, and M. Bichler, Phys. Rev. Lett. **83**, 804 (1999).
[9] F. R. Waugh, M. J. Berry, D. J. Mar, R. M. Westervelt, K. L. Campman, and A. C. Gossard, Phys. Rev. Lett. **75**, 705 (1995).
[10] L. W. Molenkamp, K. Flensberg, and M. Kemerink, Phys. Rev. Lett. **75**, 4282 (1995).
[11] M. Taut, Phys. Rev. B **62**, 8126 (2000).
[12] G. Burkard, G. Seelig, and D. Loss, Phys. Rev. B **62**, 2581 (2000).
[13] K. Mukai, S. Abe, and H. Sumi, J. Phys. Chem. B **103**, 6096 (1999).
[14] Z. K. Tang, A. Yanase, T. Yasui, Y. Segawa, and K. Cho, Phys. Rev. Lett. **71**, 1431 (1993).
[15] N. Sakakura and Y. Masumoto, Phys. Rev. B **56**, 4051 (1997).
[16] A. I. Ekimov, Al. L. Eflos, and A. A. Onushchenko, Solid State Commun. **56**, 921 (1985).
[17] T. Itoh, S. Yano, N. Katagiri, Y. Iwabuchi, C. Gourdon, and A. I. Ekimov, J. Lumin. **60&61**, 396 (1994).
[18] K. Kobayashi, S. Sangu, H. Ito, and M. Ohtsu, Phys. Rev. A **63**, 013806 (2001).
[19] T. Kataoka, T. Tokizaki, and A. Nakamura, Phys. Rev. B **48**, 2815 (1993).
[20] T. Suzuki, T. Mitsuyu, K. Nishi, H. Ohyama, T. Tomimasu, S. Noda, T. Asano, and A. Sasaki, Appl. Phys. Lett. **69**, 4136 (1996).
[21] T. Saiki, S. Mononobe, M. Ohtsu, N. Saito, and J. Kusano, Appl. Phys. Lett. **68**, 2612 (1996).
[22] T. Saiki and K. Matsuda, Appl. Phys. Lett. **74**, 2773 (1999).